

Article

Effect of Electrochemical Pre-Oxidation for Mitigating Ultrafiltration Membrane Fouling Caused by Extracellular Organic Matter

Shunkai Xu ^{1,2}, Guangchao Li ^{1,*} , Shiqing Zhou ¹, Zhou Shi ¹ and Bin Liu ¹ 

- ¹ Key Laboratory of Building Safety and Energy Efficiency, Ministry of Education, Department of Water Engineering and Science, College of Civil Engineering, Hunan University, Changsha 410082, China; skxu@hnu.edu.cn (S.X.); sqzhou@hnu.edu.cn (S.Z.); zhous61@163.com (Z.S.); ahxclb@163.com (B.L.)
- ² Beijing General Municipal Engineering Design & Research Institute Co., Ltd., Beijing 100081, China
- * Correspondence: lgc_hnu@hnu.edu.cn

Abstract: Algal extracellular organic matter (EOM) will cause grievous membrane fouling during the filtration of algae-laden water; hence, boron-doped diamond (BDD) anodizing was selected as the pretreatment process before the ultrafiltration, and the EOM fouling mitigation mechanism and the purification efficiency were systematically investigated. The results showed that BDD oxidation could significantly alleviate the decline of membrane flux and reduce membrane fouling, and the effect was more notable with an increase in oxidation time. Less than 10% flux loss happened when oxidation duration was 100 min. The dominant fouling model was gradually replaced by standard blocking. BDD anodizing preferentially oxidizes hydrophobic organic matter and significantly reduces the DOC concentration in EOM. The effluent DOC was reduced to less than 1 mg/L when 100 min of BDD anodizing was applied. After the pre-oxidation of BDD, the zeta potential and interfacial free energy, including the cohesive and adhesive free energy, were all constantly increasing, which implied that the pollutants would agglomerate and deposit, and the repulsion between foulants and the ultrafiltration membrane was augmented with the extensive oxidation time. This further confirms the control of BDD on membrane fouling. In addition, the BDD anodizing coupled ultrafiltration process also showed excellent performance in removing disinfection by-product precursors.



Citation: Xu, S.; Li, G.; Zhou, S.; Shi, Z.; Liu, B. Effect of Electrochemical Pre-Oxidation for Mitigating Ultrafiltration Membrane Fouling Caused by Extracellular Organic Matter. *Water* **2023**, *15*, 2235. <https://doi.org/10.3390/w15122235>

Academic Editor: Andreas Angelakis

Received: 12 May 2023
Revised: 3 June 2023
Accepted: 13 June 2023
Published: 14 June 2023



Copyright: © 2023 by the authors. Licensee MDPI, Basel, Switzerland. This article is an open access article distributed under the terms and conditions of the Creative Commons Attribution (CC BY) license (<https://creativecommons.org/licenses/by/4.0/>).

Keywords: BDD electrode; ultrafiltration; EOM; fouling mitigation; DBP control

1. Introduction

Algal blooms caused by water eutrophication are a great threat to people's living environments and drinking water safety. It will not only cause unpleasant taste and odor but also release various toxic and harmful substances, such as disinfection by-product precursors and microcystin, which are stable in the water environment and difficult to remove by conventional processes [1,2]. The ultrafiltration process is widely applied to water treatment for its excellent solid–liquid separation performance, and it has a good purification impact on algae-containing water by size exclusion without destroying algal cells [3]. However, the severe membrane fouling problem caused by algae limits the development of the ultrafiltration process. Membrane fouling not only increases the membrane resistance and operating cost and reduces the water production efficiency, but also decreases the service life of the membrane, so research on membrane fouling control is always the goal of our unremitting exploration [4].

The dominant cause of membrane fouling is organic matter released by algae, especially extracellular organic matter (EOM) [3,5]. Numerous studies show that the main components of EOM are protein, polysaccharide, and humus, among which polymers and hydrophilic substances account for the majority [3,6,7]. A large number of algal cells are trapped on the membrane surface when the ultrafiltration process is used to treat

algae-containing water, resulting in serious pollution of the filter cake layer, which leads to a rapid decline in membrane flux. Moreover, EOM will fill the void of the filter cake layer composed of algal cells, and the sticky EOM will reinforce the bonding of algal cell particles to each other, causing a more severe flux decrease [8,9].

Many strategies have been explored to control membrane fouling, such as adjusting the operating parameters of the membrane treatment process, modifying the properties of the membrane, and adding a pretreatment [10]. Coupling the pretreatment, including oxidation, coagulation, and adsorption, prior to the membrane process, is an effective way to control membrane fouling, and pre-oxidation is always an ideal choice among various pretreatment technologies [11]. Wan et al. [12] comparatively studied the efficacy of ultrafiltration with various ultraviolet-based advanced oxidation processes (UV-AOPs) and pretreatment technologies, including UV/persulfate, UV/chlorine, and UV/H₂O₂, in treating algae-containing water. The results showed that UV/persulfate pretreatment had the best membrane-fouling mitigation effect, followed by UV/H₂O₂ pretreatment, and with the increase in oxidant dosage, the fouling mitigation performance was improved. However, UV/chlorine aggravated the membrane pollution and caused irreversible pollution resistance through the accumulation of hydrophobic organic compounds on the membrane surface. Zhu et al. [13] studied the effect of peracetic acid (PAA), UV/PAA, and ultrasonic/PAA oxidation on ultrafiltration performance during algae-laden water treatment and found that EOM degradation was the dominant mechanism for fouling mitigation and the primary negative factor for the filtration was cell rupture rather than IOM release.

Electrochemical oxidation technology, as a new environmentally friendly water treatment technology, has wide application prospects because of its low polluting effects, high removal efficiency, and mild operating conditions [14]. Compared with algae removal by adding oxidants, electrochemical oxidation will not produce secondary pollution, and it can simultaneously remove organic pollutants in algae-containing water during electrolysis [15]. The boron-doped diamond (BDD) electrode is a new type of high-efficiency multifunctional electrode with a very wide electrochemical potential window, a small background current, and good chemical inertness of the diamond. It is suitable for the treatment of high concentration, strong acid–base, high toxicity, and refractory organic wastewater, for killing and eliminating viruses and bacteria, and is an ideal choice of electrochemical electrode materials [16]. Long et al. [17] utilized the electrochemical system with a boron-doped diamond (BDD) anode and carbon felt (CF) cathode to remove *Microcystis aeruginosa*, and the removal performance of BDD-CF electrodes was significantly improved via the addition of Fe²⁺. Liu et al. [18] reported that BDD anodizing could effectively alleviate membrane fouling derived from algae with an oxidation time of over 30 min. Hence, BDD anodizing is an effective way to reduce membrane fouling in algae-containing water treatment. This study used a BDD anode and extracellular organic matter (EOM) in algae-containing water as target pollutants to further analyze and explore the mechanism of action of algal organic matter on an ultrafiltration membrane.

In this work, the influence of the degree of pre-oxidation on the ultrafiltration process was explored by setting different oxidation times. By studying membrane fouling reversibility and the membrane flux curve, the mechanism of action of algae-derived organic matter on the ultrafiltration membrane was analyzed and explored. Additionally, the fouling model and foulant properties, including zeta potential, hydrophilicity, and interfacial free energy, were investigated. Finally, the effect of BDD oxidation on the purification performance of DOC and disinfection by-product precursors was studied.

2. Materials and Method

2.1. EOM Extraction

Microcystis aeruginosa was employed for EOM preparation. The algae seeds were obtained from the Institute of Hydrobiology, Chinese Academy of Sciences. The detailed cultivation method for *Microcystis aeruginosa* can be found in our previous works [19]. The

algae in the stationary phase with 35 harvesting days was employed for EOM extraction. A refrigerated centrifuge was utilized for the extraction, and the temperature (4 °C) and rotation speed (10,000 rpm) were fixed for 20 min. The supernatant was separated with algae on the centrifuge tube wall and then filtrated with a 0.45 µm microfiltration membrane. Finally, the dissolved organic carbon (DOC) of the EOM was adjusted to 5 mg/L with 15.0 mM NaClO₄ [18].

2.2. Experimental Protocol

An electrochemical experimental apparatus and a flat-sheet, dead-end UF module constituted the combined ultrafiltration treatment protocol. The electrochemical experimental apparatus specifically included a power supply, electrode, electrolytic cell, and stirring device, and the schematic diagram is depicted in Figure 1a. The power was provided by a DC power supply, and the current was stabilized at 0.3 A. The anode was a BDD electrode, and the cathode was a titanium electrode. The distance between the two electrodes was 10 mm, and the electrode plate area was 10 cm²; hence, the current density of the electrochemical device was 30 mA/cm². The amount of EOM treated in the electrolysis cell was 200 mL each time, and a magnetic stirrer was employed during the electrolysis process to promote mass transfer. In this work, the electro-oxidation time was set to 0 min, 10 min, 30 min, 60 min, and 100 min in order to explore the influence of different electro-oxidation times on the treatment of the EOM solution.

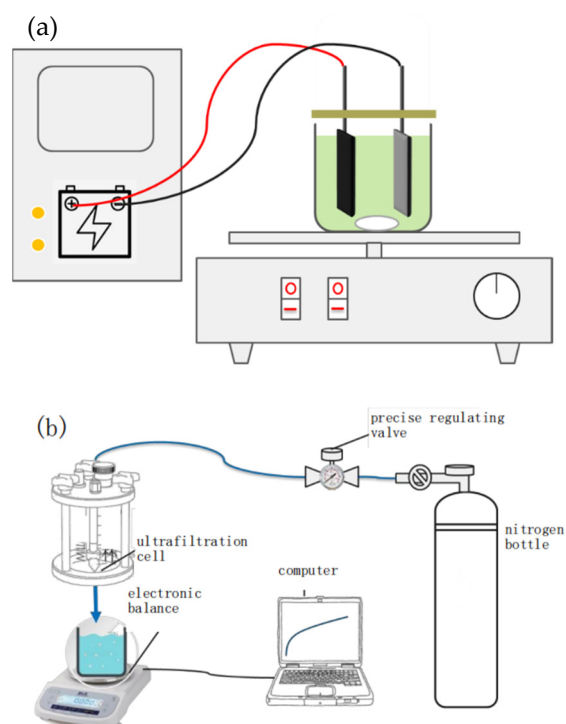


Figure 1. Schematic diagram of electrochemical experimental apparatus, (a) electrochemical experimental apparatus; (b) membrane fouling assessment.

The flat-sheet, dead-end UF module was employed for the membrane fouling assessment, as shown in Figure 1b. The ultrafiltration system specifically included an UF cell (UFSC05001, Millipore, Burlington, MA, USA), electronic balance (NV2201ZH, Ohaus, Parsippany, NJ, USA), a high-pressure nitrogen bottle with stable output pressure of 100 kPa that passed through a precise regulating valve, and a computer terminal. The samples, after different durations of electrochemical treatment, were directly filtered by the membrane. The water in the ultrafiltration cell flowed through the silicone tube into the beaker placed on the balance, and the electronic balance was connected to the computer to record the

water output data in real time, at a frequency of once every 5 s. Then, the flux curve for the ultrafiltration process was drawn.

2.3. Membrane Fouling Assessment

According to the series resistance model based on Darcy’s law, the membrane fouling resistance during the filtration process was calculated [7,12]. Equation (1) shows that the total membrane resistance R_{tot} was composed of membrane inherent resistance R_m , reversible resistance R_r , and irreversible resistance R_{ir} .

$$J = \frac{\Delta P}{\mu(R_m + R_r + R_{ir})} \tag{1}$$

where J represents membrane flux, ΔP represents transmembrane pressure difference (Pa), and μ is dynamic viscosity (Pa·s).

First, ultrapure water was used to filter until the membrane flux was stable, which was recorded as J_0 , and the membrane inherent resistance R_m was obtained by taking J_0 into Equation (2).

$$R_m = \frac{\Delta P}{\mu J_0} \tag{2}$$

Then, the average filtration flux of the last 1 mL was calculated as J_1 , and the total membrane fouling resistance R_{tot} could be obtained accordingly using Equation (3).

$$R_{tot} = \frac{\Delta P}{\mu J_1} \tag{3}$$

After the algae-containing water was filtered, we gently wiped the surface of the ultrafiltration membrane with a wet sponge, then placed the ultrafiltration membrane at the bottom of ultrafiltration cell again, sequentially filtering with ultrapure water, and recorded the steady flux J_2 . Hence, the irreversible resistance R_{ir} and reversible resistance R_r could be calculated according to Equations (4) and (5).

$$R_{ir} = \frac{\Delta P}{\mu J_2} - \frac{\Delta P}{\mu J_0} \tag{4}$$

$$R_r = R_{tot} - R_m - R_{ir} \tag{5}$$

Hermia described four classical pollution models, including a complete blocking model [20], a standard blocking model, a critical blocking model, and a filter cake layer model (Table 1). It is generally considered that the fouling caused by the standard blocking process occurs in the membrane pores, which is irreversible pollution, while the pollution caused by the complete blocking, intermediate blocking, and filter cake layer blocking processes occurs on the membrane surface, which is usually reversible pollution.

Table 1. Four classical fouling models.

Fouling Model	Equation	n
Cake layer filtration	$\frac{1}{J} - \frac{1}{J_0} = AV$	0
Critical blocking	$\frac{1}{J} + B = \frac{J_0}{V}$	1
Standard blocking	$\ln J_0 - \ln J = CV$	1.5
Complete blocking	$J_0 - J = DV$	2

Note: where J_0 is the initial flux; t is the filter time; V is the filtrated volume; A , B , C , and D are constant.

The value of n was calculated as follows [21]: dt/dV was calculated using membrane flux data based on Equation (7), and d^2t/dV^2 was calculated using dJ/dt (Equation (8)), which was obtained by calculating the differential relationship between flux and time with

Matlab[®] 2014 software. Then, the n value could be obtained by calculating the logarithmic relationship between the dt/dV and d^2t/dV^2 according to Equation (9) [22].

$$\frac{d^2t}{dV^2} = k \left(\frac{dt}{dV} \right)^n \quad (6)$$

$$\frac{dt}{dV} = \frac{1}{JA} \quad (7)$$

$$\frac{d^2t}{dV^2} = -\frac{1}{J^3 A^2} \frac{dJ}{dt} \quad (8)$$

$$n = \frac{d \left[\log \left(\frac{d^2t}{dV^2} \right) \right]}{d \left[\log \left(\frac{dt}{dV} \right) \right]} \quad (9)$$

2.4. Analytical Methods

In this experiment, dissolved organic carbon (DOC) was detected using a total organic carbon analyzer (JC-CD-800, Shimadzu, Duisburg, Germany), and a nanometer particle size analyzer (S90, Malvern Instruments Ltd., Malvern, UK) was used to measure the zeta potential on the surfaces of algal cells, which reflects the changing situation and characteristics of aggregation and sedimentation of algal cells. The contact angle was measured with a contact angle meter (Theta Lite, Beijing, China), and diiodomethane, ultrapure water, and glycerol were utilized as test liquids to calculate the interface free energy on the basis of XDLVO theory [23].

The nonionic XAD resin, including XAD-4 and XAD-8 (Mberlite, Rohm Haas, Tianjin, China), was used to separate organic substances with different hydrophilicities and hydrophobicities in the algae-laden water. Gas chromatography/mass spectrometry (GC/MS) was used to determine the precursors of disinfection by-products [18]. Unless otherwise specified, all the water quality indicators in this experiment were tested three times in parallel to control the experimental errors and ensure the reliability and scientificity of the data.

3. Results and Discussion

3.1. Effect of Electrochemical Pre-Oxidation on Membrane Fouling Reversibility

The relative flux reduction (RFR) during filtration of EOM due to adsorptive fouling is illustrated in Figure 2. The RFR of the EOM solution without electrochemical pre-oxidation was 36.7%, which indicates that the adhesion potential of EOM onto the PVDF membrane was great. This was also consistent with previously reported work [24]. When the BDD anodizing duration was 10 min, the RFR reversibly ascended. This may be because the small molecular organics generated at 10 min had a higher potential to penetrate into or adsorb onto the membrane.

The effect of the BDD anode electro-oxidation on the flux drop of the PVDF membrane during filtration of EOM is shown in Figure 3. It can be observed that the flux curve of direct filtration (0 min) was highly declining. The specific flux of direct filtrate declined to 0.36 at the end of the filtration, which indicates that the EOM had strong fouling potential. This was in accordance with previous research that found that algae-laden water adversely affected the operation of ultrafiltration. However, the flux decline was obviously improved when the BDD anode was employed as the pre-oxidation method. After 10 min of electrochemical pre-oxidation, the specific flux was apparently alleviated, and the specific flux dropped to about 0.5 at the end of the filtration. When we continued to extend the pre-oxidation duration, the specific flux curve of EOM was further improved. The specific flux was slightly decreased to 0.81 when the oxidation duration was extended to 60 min, and less than 10% flux loss occurred when the oxidation duration was 100 min. This shows that the BDD anode pre-oxidation treatment was a valid way of alleviating the fouling of algae-

derived organics, which can probably be attributed to the oxidation, decomposition, and even mineralization of organic substances, thus greatly reducing membrane foulant load during the UF process [25].

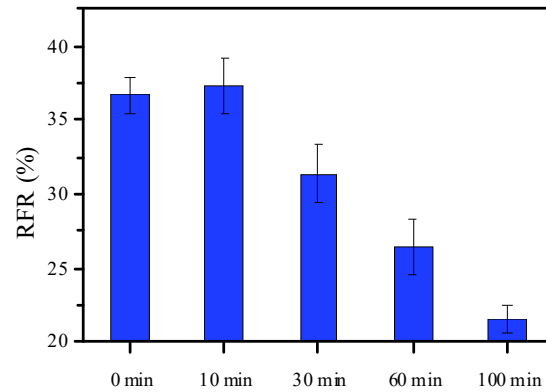


Figure 2. Adsorptive fouling of the PVDF ultrafiltration membrane under different pre-oxidation durations.

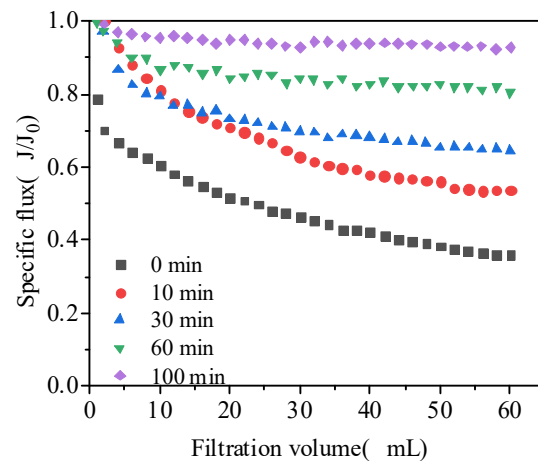


Figure 3. Flux curve under different pre-oxidation durations.

The effect of BDD pre-oxidation duration on the membrane fouling reversibility of the UF membrane is presented in Figure 4. The weight of reversible fouling resistance caused by cake layer formation in total fouling resistance exceeded the weight of irreversible fouling caused by pore blocking, regardless of the electro-oxidation duration. Though a similar result was also reported during the ultrafiltration process during algae-laden water treatment, the proportion of irreversible fouling resistance was much higher during the treatment of the EOM. The fouling caused by algae cell deposition is probably the reason for this differentiation. It can be noted that both reversible and irreversible fouling were notably mitigated when the pretreatment duration was extended. This was not in accordance with the results of adsorptive fouling with different pre-oxidation durations, which might indicate that the adsorptive fouling could account for a quite limited portion of the total fouling resistance. For instance, the irreversible fouling resistance reduced to $0.14 \times 10^{12} \text{ m}^{-1}$, and the reversible fouling resistance declined to $3.36 \times 10^{12} \text{ m}^{-1}$ when 100 min of anodizing oxidation was applied. The irreversible fouling resistance and the reversible fouling resistance dropped by 95% and 43%, respectively, compared with direct filtration. This indicates that both reversible and irreversible fouling, especially irreversible fouling, could be greatly alleviated by the BDD anodizing pretreatment. In general, the rapid rise of irreversible fouling was unfavorable for the operation of ultrafiltration because the hydraulic washing was limited by the ease of irreversible fouling. Hence, anodizing the BDD prior to UF was an efficacious strategy for membrane fouling control [18].

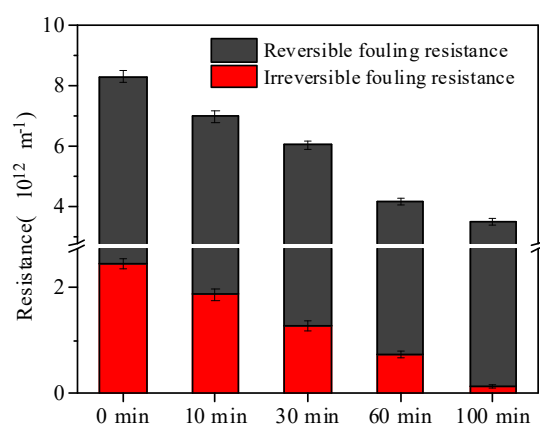


Figure 4. Fouling resistance of the PVDF membrane under different pre-oxidation durations.

A two-stage fouling model was employed to investigate the membrane fouling mechanism under various pre-oxidation durations. As illustrated in Table 1, the n value (linear fitting correlation slope value) reflected the dominant fouling mechanism. Additionally, if the n value was located between the n values corresponding to two fouling mechanisms, it suggests that the fouling mechanisms were both dominant. The fitting curve on the basis of d^2t/dV^2 and dt/dV during the filtration process is illustrated in Figure 5. The results show that the direct filtration of EOM was in line with a typical two-stage fitting curve, which indicates that critical blocking and standard blocking were the dominant fouling mechanisms during the initial filtration period, while cake layer filtration surpassed and governed the fouling mechanism with continuous filtration. The two-stage fitting curve still existed when 10 min and 30 min electrochemistry pre-oxidation were utilized. However, a one-stage fitting curve emerged when the pre-oxidation duration was longer than 60 min. When the pre-oxidation duration was 60 min or 100 min, the standard blocking was the dominant fouling mechanism. This suggests that critical blocking was gradually replaced by standard blocking when the oxidation time increased from 10 min to 100 min [26]. This was probably because, with the prolonging of the pre-oxidation duration, more macromolecular organic matter was degraded into small molecules. Then, those small molecules were prone to penetrating into the membrane pores and generating fouling in the membrane tunnel, i.e., standard blocking. Additionally, based on the analysis of fouling irreversibility (Figure 3), it can be verified that, though cake layer fouling was not dominant when the oxidation duration was longer than 60 min, reversible fouling potential still accumulated.

3.2. Effect of Electrochemical Pre-Oxidation on Foulant Property

To further investigate the effects of the BDD anodizing pretreatment on foulant characteristics, foulants with solution and interfacial conditions were detected. The zeta potential was employed to characterize the stability of dispersion (Table 2). The zeta potential of the untreated EOM solution was -19.1 mV, which indicates that the organics of the EOM show a stable state. When pre-oxidation was employed, the zeta potential of the EOM solution started to decline, which indicates that the solution tends to be unstable when BDD anodizing is utilized. Additionally, with a longer oxidation duration, the decline of zeta potential was more significant. This suggests that the BDD oxidation process not only caused a decrease in the molecular weight of the organic matter but also the disappearance of the stable state of the organic matter. A previous study determined that the fouling layer formed by a labile foulant had lower resistance and was easier to remove [27]. Hence, the zeta potential of the feed solution under various pre-oxidation durations was in accordance with the filtration performance.

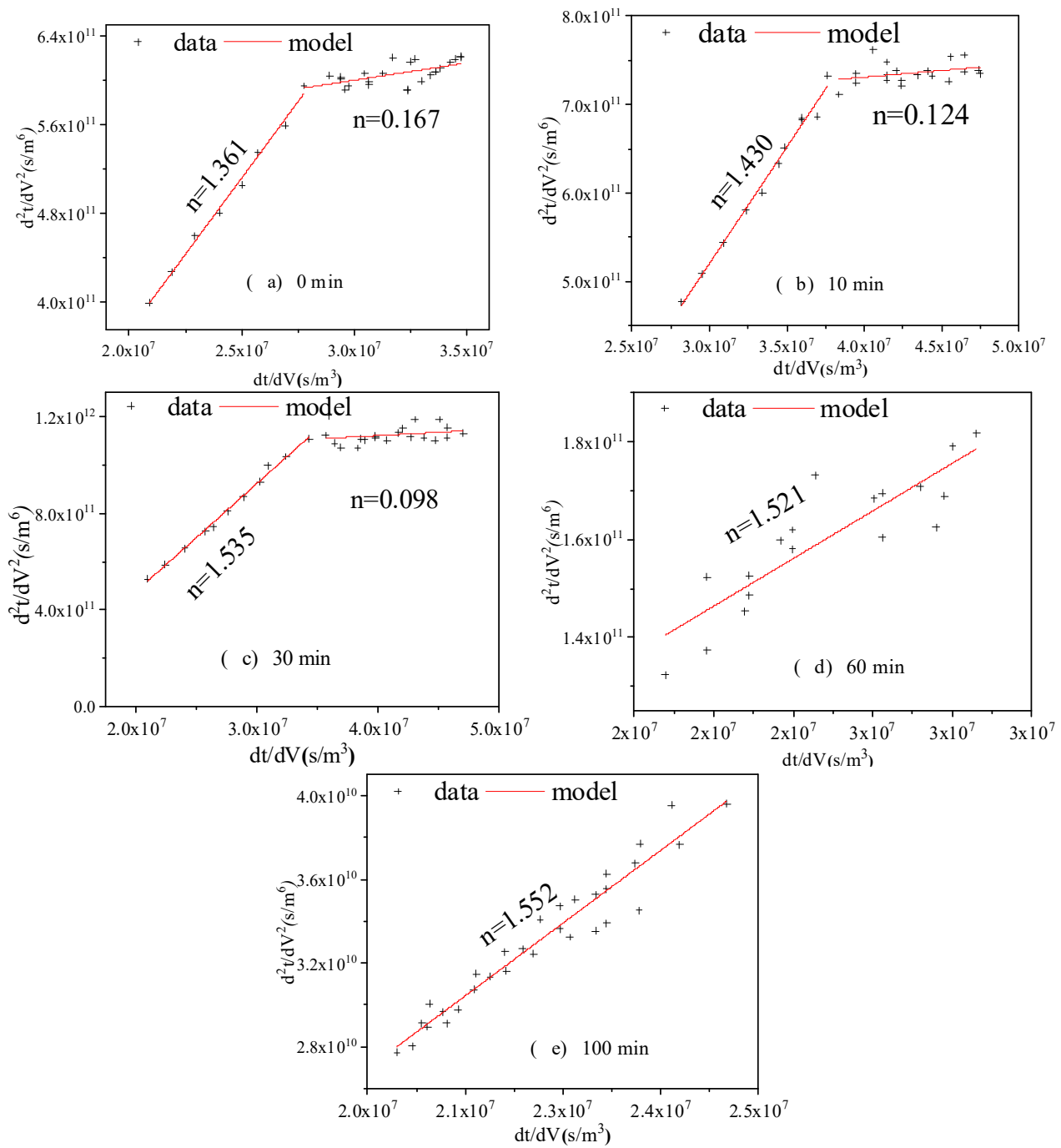


Figure 5. Data and fitting curve (d^2t/dV^2 and dt/dV) under different pre-oxidation durations.

Table 2. Zeta potential of feed solution under different pre-oxidation durations.

Pre-Oxidation Time	Zeta Potential
0 min	−19.1 mV
10 min	−18.6 mV
30 min	−17.8 mV
60 min	−15.4 mV
100 min	−14.9 mV

The hydrophilicity of the EOM with different pre-oxidation durations was also investigated. Figure 6 presents the hydrophobic, transition, and hydrophilic classifications of the

EOM solution after oxidation and ultrafiltration, respectively. It can be seen from the figure that the proportion of hydrophilic content comprised the overwhelming majority of the EOM solution, which was consistent with the previous reported works. During the direct UF process, the hydrophobic, transition, and hydrophilic content were respectively reduced by 26.2%, 16.1%, and 18.8%. The superior removal efficiency of the hydrophobic organics was probably because macromolecular organics are more hydrophobic and hence easier to intercept by the membrane. On the other hand, the degradation ratio of the hydrophobic component by BDD anodizing was significantly greater than that of the hydrophilic component. A possible reason for this phenomenon is that hydrophobic macromolecular organics were prone to being transformed into hydrophilic micromolecular organics. In general, though both anodization and ultrafiltration contributed to the removal of organic matter, the degradation by BDD anodizing was more distinguished than the ultrafiltration rejection, especially when the oxidation duration was extended.

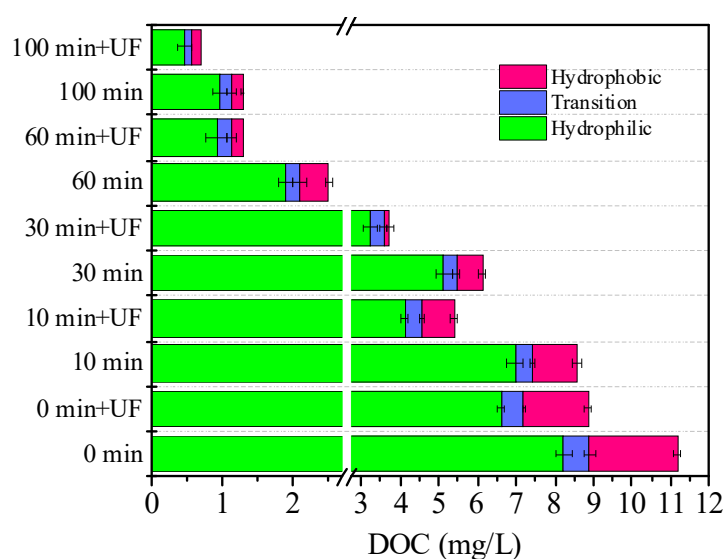


Figure 6. Hydrophilic and hydrophobic classification of feed and effluent under different pre-oxidation durations.

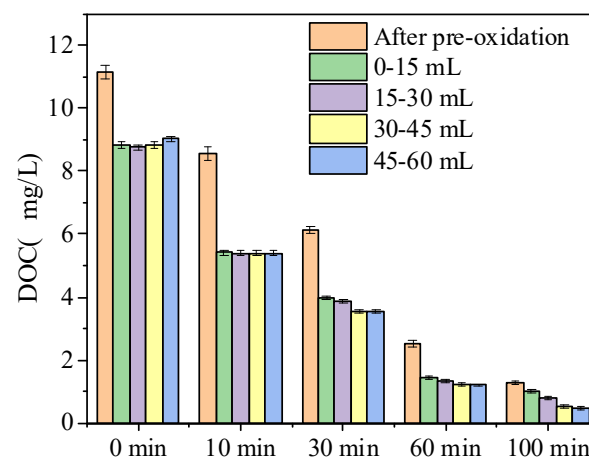
The cohesive and adhesive free energies of the fouled PVDF ultrafiltration membrane under various pre-oxidation durations are listed in Table 3. The total interface free energy, regardless of whether it was cohesive or adhesive, was calculated by the sum of the Van der Waals interaction, polar interaction, and electrostatic interaction. Mostly, the Van der Waals interaction and polar interaction were dominant when compared to the electrostatic interaction. As observed from the table, both cohesive and adhesive free energy obviously declined after BDD anodizing. The cohesive free energy decreased from -16.32 mJ/m^2 to -6.11 mJ/m^2 after 100 min of pre-oxidation, while the adhesive free energy sharply decreased from -68.65 mJ/m^2 to -9.16 mJ/m^2 after 100 min of pre-oxidation. The declining trend of cohesive free energy was positively correlated with the zeta potential, which suggests the stabilities of the foulants were in line with the interaction between foulant and foulant regardless of whether it occurred in the feed solution or on the membrane surface. On the other hand, the decline of adhesive free energy was much more significant when pre-oxidation was utilized. This suggests that the repulsive force was enhanced when BDD anodizing was employed. Hence, a cake layer with lower resistance can be easily removed after the pretreatment.

Table 3. Free energy of PVDF ultrafiltration membrane surface under different pre-oxidation durations.

		0 min	10 min	30 min	60 min	100 min
Cohesive free energy	G_{131}^{TOT}	−16.32	−15.85	−12.67	−6.57	−6.11
Adhesive free energy	G_{132}^{TOT}	−68.65	−51.33	−32.22	−18.67	−9.16

3.3. Effect of Electrochemical Pre-Oxidation on Separation Performance

The DOC removal efficiency of the membrane with various pre-oxidation durations is shown in Figure 7. The rejection of the PVDF membrane on DOC during direct filtration was 20.6%. Additionally, the fluctuation of effluent DOC during various filtration periods was small. Previous studies confirm that two factors could influence the separation performance in different filtration periods. One factor is membrane adsorption during the initial filtration period. In the beginning period, some of the hydrophobic matter could be adsorbed by the membrane, and hence, the DOC rejection was enhanced; however, the adsorption of the membrane was usually valid for a limited period until the membrane adsorption was saturated. Another factor is the enhanced separation effect of a dense cake layer, in which the separation performance was negatively related to the cake layer fouling, i.e., the “trade-off” effect. Mostly, the cake layer could obviously enhance the separation performance of ultrafiltration during treatment of algae-laden water due to its high cake layer resistance. The DOC rejection of the membrane with 10 min to 100 min of pre-oxidation duration was 37.2%, 39.1%, 48.7%, and 46.5%, respectively. This suggests that the BDD anodizing could greatly increase the organic removal efficiency. Moreover, when the oxidation duration was 100 min, the effluent DOC concentration was below 1 mg/L, which indicates excellent water quality in terms of total organic content.

**Figure 7.** Removal of DOC by the PVDF ultrafiltration membrane under different pre-oxidation durations.

The disinfection by-product precursors of chlorine- and algae-derived toxins after oxidation and membrane filtration were both detected in addition to total organic indicators. As shown in Figure 8, the trichloromethane formation potential and microcystin-LR (MCLR) were used to investigate the DBP and toxin rejection efficacy of the BDD anodizing-enhanced ultrafiltration process. The concentration of TCMFP in EOM was 46.73 $\mu\text{g/L}$, and it sharply declined to 36.77 $\mu\text{g/L}$, 20.85 $\mu\text{g/L}$, 14.82 $\mu\text{g/L}$, and 11.50 $\mu\text{g/L}$ during the BDD anodizing durations of 10 min, 30 min, 60 min, and 100 min, respectively. This indicates that the control of DBPs by BDD electro-oxidation was achieved with high efficiency when the oxidation duration longer than 60 min and the TCMFP concentration was lower than 15 $\mu\text{g/L}$. Moreover, the TCMFP concentration of effluent after membrane filtration was 4.07 $\mu\text{g/L}$, 3.47 $\mu\text{g/L}$, and 3.31 $\mu\text{g/L}$, respectively, when the oxidation durations were

30 min, 60 min, and 100 min. This suggests that electro-oxidation pretreatment coupled with ultrafiltration was an exceptional method for controlling DBP.

MCLR is the most commonly detected algae toxin in nature and is greatly hazardous to human health. In this work, the removal of MCLR by BDD pre-oxidation and membrane filtration was presented in Figure 8b. The concentration of MCLR in EOM was 5.8 $\mu\text{g/L}$, 5.3 $\mu\text{g/L}$, 3.2 $\mu\text{g/L}$, 1.5 $\mu\text{g/L}$, and 0.9 $\mu\text{g/L}$ during BDD anodizing durations of 0 min, 10 min, 30 min, 60 min, and 100 min, respectively, which suggests that BDD anodizing was an efficient way to degrade the algae-derived toxins, especially when the pre-oxidation time reached 100 min, 84% of the MCLR was removed, and the MCLR concentration was already lower than the Chinese sanitary standard for drinking water (1 $\mu\text{g/L}$). However, the further separation of MCLR by membrane was quite limited, which is distinct from the separation performance of TCMFP. This is because the molecular weight of MCLR was only 995, which was much smaller than the UF molecular weight cutoff, while some disinfection by-product precursors can be rejected by the membrane. Hence, even with superior separation performance, efficient pretreatment was still significant when considering the hazardous low-molecular-weight organics.

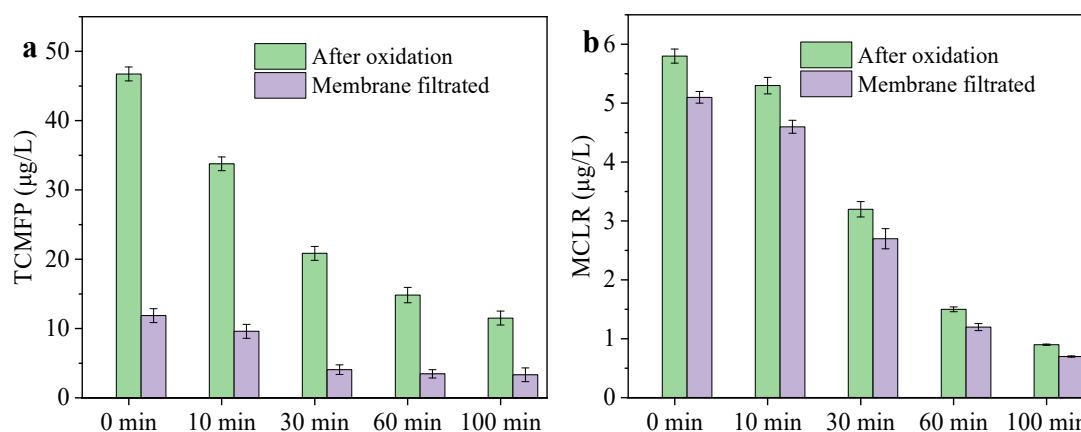


Figure 8. Removal of TCMFP (a) and MCLR (b) by the PVDF ultrafiltration membrane under different pre-oxidation durations.

4. Conclusions

In this study, BDD anodizing and ultrafiltration processes were combined to systematically explore the pretreatment efficiency of algae-laden water by combining processes with different electrochemical pre-oxidation times, including the mitigation efficiency of membrane fouling and the purification efficiency. The following main conclusions can be drawn:

- (1) BDD anodic oxidation can effectively alleviate the membrane flux decline and irreversible membrane fouling by oxidizing and removing organic substances in EOM, and the critical blocking is gradually replaced by the standard blocking as the oxidation time increases;
- (2) BDD anodic oxidation can increase the zeta potential of EOM and interfacial free energy, which promotes the destabilization and sedimentation of the EOM solution;
- (3) Electrochemical pre-oxidation and ultrafiltration processes both have excellent removal performance for the disinfection by-product precursors.

Author Contributions: Validation, G.L.; Resources, S.Z.; Writing—original draft, S.X.; Writing—review & editing, Z.S.; Funding acquisition, B.L. All authors have read and agreed to the published version of the manuscript.

Funding: This work was financially supported by National Natural Science Foundation Youth Fund (52200015).

Data Availability Statement: Data available on request.

Conflicts of Interest: The authors declare no conflict of interest.

References

1. Fang, J.Y.; Yang, X.; Ma, J.; Shang, C.; Zhao, Q.A. Characterization of algal organic matter and formation of DBPs from chlor(am)ination. *Water Res.* **2010**, *44*, 5897–5906. [[CrossRef](#)] [[PubMed](#)]
2. Qu, F.S.; Liang, H.; He, J.G.; Ma, J.; Wang, Z.Z.; Yu, H.R.; Li, G.B. Characterization of dissolved extracellular organic matter (dEOM) and bound extracellular organic matter (bEOM) of *Microcystis aeruginosa* and their impacts on UF membrane fouling. *Water Res.* **2012**, *46*, 2881–2890. [[CrossRef](#)] [[PubMed](#)]
3. Gao, K.; Li, T.; Zhao, Q.Q.; Liu, W.; Liu, J.X.; Song, Y.L.; Chu, H.Q.; Dong, B.Z. UF fouling behavior of allelopathy of extracellular organic matter produced by mixed algae co-cultures. *Sep. Purif. Technol.* **2021**, *261*, 11. [[CrossRef](#)]
4. Guo, W.S.; Ngo, H.H.; Li, J.X. A mini-review on membrane fouling. *Bioresour. Technol.* **2012**, *122*, 27–34. [[CrossRef](#)]
5. Villacorte, L.O.; Tabatabai, S.A.A.; Anderson, D.M.; Amy, G.L.; Schippers, J.C.; Kennedy, M.D. Seawater reverse osmosis desalination and (harmful) algal blooms. *Desalination* **2015**, *360*, 61–80. [[CrossRef](#)]
6. Henderson, R.K.; Baker, A.; Parsons, S.A.; Jefferson, B. Characterisation of algogenic organic matter extracted from cyanobacteria, green algae and diatoms. *Water Res.* **2008**, *42*, 3435–3445. [[CrossRef](#)]
7. Qu, F.S.; Liang, H.; Wang, Z.Z.; Wang, H.; Yu, H.R.; Li, G.B. Ultrafiltration membrane fouling by extracellular organic matters (EOM) of *Microcystis aeruginosa* in stationary phase: Influences of interfacial characteristics of foulants and fouling mechanisms. *Water Res.* **2012**, *46*, 1490–1500. [[CrossRef](#)]
8. Babel, S.; Takizawa, S. Microfiltration membrane fouling and cake behavior during algal filtration. *Desalination* **2010**, *261*, 46–51. [[CrossRef](#)]
9. Her, N.; Amy, G.; Park, H.R.; Song, M. Characterizing algogenic organic matter (AOM) and evaluating associated NF membrane fouling. *Water Res.* **2004**, *38*, 1427–1438. [[CrossRef](#)] [[PubMed](#)]
10. Huang, H.; Schwab, K.; Jacangelo, J.G. Pretreatment for Low Pressure Membranes in Water Treatment: A Review. *Environ. Sci. Technol.* **2009**, *43*, 3011–3019. [[CrossRef](#)] [[PubMed](#)]
11. Cheng, X.X.; Liang, H.; Ding, A.; Qu, F.S.; Shao, S.L.; Liu, B.; Wang, H.; Wu, D.J.; Li, G.B. Effects of pre-ozonation on the ultrafiltration of different natural organic matter (NOM) fractions: Membrane fouling mitigation, prediction and mechanism. *J. Membr. Sci.* **2016**, *505*, 15–25. [[CrossRef](#)]
12. Wan, Y.; Xie, P.C.; Wang, Z.P.; Ding, J.Q.; Wang, J.W.; Wang, S.L.; Wiesner, M.R. Comparative study on the pretreatment of algae-laden water by UV/persulfate, UV/chlorine, and UV/H₂O₂: Variation of characteristics and alleviation of ultrafiltration membrane fouling. *Water Res.* **2019**, *158*, 213–226. [[CrossRef](#)] [[PubMed](#)]
13. Zhu, T.T.; Liu, B. Mechanism study on the effect of peracetic acid (PAA), UV/PAA and ultrasonic/PAA oxidation on ultrafiltration performance during algae-laden water treatment. *Water Res.* **2022**, *220*, 11. [[CrossRef](#)] [[PubMed](#)]
14. Park, H.; Choo, K.H.; Park, H.S.; Choi, J.; Hoffmann, M.R. Electrochemical oxidation and microfiltration of municipal wastewater with simultaneous hydrogen production: Influence of organic and particulate matter. *Chem. Eng. J.* **2013**, *215*, 802–810. [[CrossRef](#)]
15. Qiao, J.; Xiong, Y.Z. Electrochemical oxidation technology: A review of its application in high-efficiency treatment of wastewater containing persistent organic pollutants. *J. Water Process. Eng.* **2021**, *44*, 25. [[CrossRef](#)]
16. Yu, X.M.; Zhou, M.H.; Hu, Y.S.; Serrano, K.G.; Yu, F.K. Recent updates on electrochemical degradation of bio-refractory organic pollutants using BDD anode: A mini review. *Environ. Sci. Pollut. Res.* **2014**, *21*, 8417–8431. [[CrossRef](#)]
17. Long, Y.J.; Li, H.N.; Xing, X.; Ni, J.R. Enhanced removal of *Microcystis aeruginosa* in BDD-CF electrochemical system by simple addition of Fe²⁺. *Chem. Eng. J.* **2017**, *325*, 360–368. [[CrossRef](#)]
18. Liu, B.; Zhu, T.T.; Liu, W.K.; Zhou, R.; Zhou, S.Q.; Wu, R.X.; Deng, L.; Wang, J.; Van der Bruggen, B. Ultrafiltration pre-oxidation by boron-doped diamond anode for algae-laden water treatment: Membrane fouling mitigation, interface characteristics and cake layer organic release. *Water Res.* **2020**, *187*, 11. [[CrossRef](#)]
19. Liu, B.; Qu, F.S.; Chen, W.; Liang, H.; Wang, T.Y.; Cheng, X.X.; Yu, H.R.; Li, G.B.; Van der Bruggen, B. *Microcystis aeruginosa*-laden water treatment using enhanced coagulation by persulfate/Fe(II), ozone and permanganate: Comparison of the simultaneous and successive oxidant dosing strategy. *Water Res.* **2017**, *125*, 72–80. [[CrossRef](#)]
20. Hermia, J. Constant Pressure Blocking Filtration Laws-Application to Power-Law Non-Newtonian Fluids. *Trans. Inst. Chem. Eng.* **1982**, *60*, 183–187.
21. Ho, C.C.; Zydny, A.L. A combined pore blockage and cake filtration model for protein fouling during microfiltration. *J. Colloid Interface Sci.* **2000**, *232*, 389–399. [[CrossRef](#)] [[PubMed](#)]
22. Lee, S.J.; Dilaver, M.; Park, P.K.; Kim, J.H. Comparative analysis of fouling characteristics of ceramic and polymeric microfiltration membranes using filtration models. *J. Membr. Sci.* **2013**, *432*, 97–105. [[CrossRef](#)]
23. Liu, B.; Qu, F.S.; Liang, H.; Gan, Z.D.; Yu, H.R.; Li, G.B.; Van der Bruggen, B. Algae-laden water treatment using ultrafiltration: Individual and combined fouling effects of cells, debris, extracellular and intracellular organic matter. *J. Membr. Sci.* **2017**, *528*, 178–186. [[CrossRef](#)]
24. Zhu, T.; Zhou, Z.; Qu, F.; Liu, B.; Van der Bruggen, B. Separation performance of ultrafiltration during the treatment of algae-laden water in the presence of an anionic surfactant. *Sep. Purif. Technol.* **2022**, *281*, 119894. [[CrossRef](#)]

25. Zhu, T.; Qu, F.; Liu, B.; Liang, H. The influence of environmental factor on the coagulation enhanced ultrafiltration of algae-laden water: Role of two anionic surfactants to the separation performance. *Chemosphere* **2022**, *291*, 132745. [[CrossRef](#)]
26. Liu, B.; Qu, F.; Yu, H.; Tian, J.; Chen, W.; Liang, H.; Li, G.; Van der Bruggen, B. Membrane fouling and rejection of organics during algae-laden water treatment using ultrafiltration: A comparison between in situ pretreatment with Fe (II)/persulfate and ozone. *Environ. Sci. Technol.* **2018**, *52*, 765–774. [[CrossRef](#)]
27. Motsa, M.M.; Mamba, B.B.; D’Haese, A.; Hoek, E.M.; Verliefde, A.R. Organic fouling in forward osmosis membranes: The role of feed solution chemistry and membrane structural properties. *J. Membr. Sci.* **2014**, *460*, 99–109. [[CrossRef](#)]

Disclaimer/Publisher’s Note: The statements, opinions and data contained in all publications are solely those of the individual author(s) and contributor(s) and not of MDPI and/or the editor(s). MDPI and/or the editor(s) disclaim responsibility for any injury to people or property resulting from any ideas, methods, instructions or products referred to in the content.